Quasi-null lens optical system for the fabrication of an oblate convex ellipsoidal mirror: application to the Wide Angle Camera of the Rosetta space mission

Maria-Guglielmina Pelizzo, Vania Da Deppo, Giampiero Naletto, Roberto Ragazzoni, and Andrea Novi

The design of a quasi-null lens system for the fabrication of an aspheric oblate convex ellipsoidal mirror is presented. The Performance and tolerance of the system have been analyzed. The system has been applied successfully for the fabrication of the primary mirror of the Wide Angle Camera (WAC), the imaging system onboard the Rosetta, the European Space Agency cornerstone mission dedicated to the exploration of a comet. The WAC is based on an off-axis two-mirror configuration, in which the primary mirror is an oblate convex ellipsoid with a significant conic constant.

OCIS codes: 350.1260, 220.1000, 120.4610.

1. Introduction

The Rosetta is the European Space Agency cornerstone mission dedicated to close observations of the 67P/Churyumov–Gerasimenko comet.[1] The Rosetta was launched in March 2004, and it will approach the comet in 2014. The probe will then orbit in the comet's gravity field and will make observations of its nucleus and coma; in addition, a Surface Science Package module will land on the comet's surface to make *in situ* observations.

The Wide Angle Camera[2,3] (WAC) and the Narrow Angle Camera[4] (NAC) are the two cameras of OSIRIS, the scientific imaging system of the probe.[5,6] During the first fly-bys the two cameras will acquire images of Mars and Earth; during the probe navigation they will collect images of asteroids; during the rendezvous with the comet they will be used to guide the Surface Science Package module's landing on the comet surface, and they will acquire images of the comet's surface, coma dust, and gas jets at different wavelengths. From a technical point of view, one of the most interesting aspects of the WAC is its optical design, based on an innovative off-axis two-mirror configuration.[3,7] In this design, the primary mirror (M1) has a convex oblate ellipsoidal surface with quite a large conic constant. One of the most challenging tasks in the camera's realization was the fabrication and characterization of this mirror.

The fabrication of an aspheric mirror is usually performed by a preliminary rough mirror shaping by means of a numerically controlled machine, followed by a fine polishing monitored by an interferometric setup: By minimizing the difference between the actual and the nominal interferogram, the correct shaping of the surface is finally obtained.[8] Interferometric testing of aspheric surfaces often requires a compensator (a null lens) element that suitably shapes the spherical or plane wave exiting the interferometer to compensate for the deformation introduced by the specific surface under test. This compensator, usually more complex than a single lens, is rather critical since it requires both an optimal manufacturing and high precision relative positioning with respect to the surface to be polished.[9] By means of this suitable tool, the optimal surface is reached when a null interferogram is obtained.

To maintain a simple and low cost, but at the same time realize a very reliable interferometric test for the fabrication of the WAC M1 mirror, we have de-

M.-G. Pelizzo (pelizzo@dei.unipd.it), V. Da Deppo, and G. Naletto are with CNR-INFM-LUXOR-Laboratory for Ultraviolet and X-ray Optical Research, Via Gradenigo, 6/B-35131, Padova, PD, Italy and with the Dipartimento di Ingegneria dell'Informazione, Via Gradenigo, 6/B-35131, Padova, PD, Italy. G. Naletto is also with CISAS-Centro Interdipartimentale Studi e Attività Spaziali G. Columbo, Via Venezia, 15-35131 Padova, PD, Italy. R. Ragazzoni is with INAF Osservatorio Astrofisico di Arcetri, Largo E. Fermi 5, 50125 Firenze, FI, Italy. A. Novi is with Galileo Avionica, Via A. Einstein 35, 50013 Campi Bisenzio, FI, Italy.

Received 3 January 2006; accepted 3 March 2006; posted 27 March 2006 (Doc. ID 67036).

0003-6935/06/246119-07$15.00/0

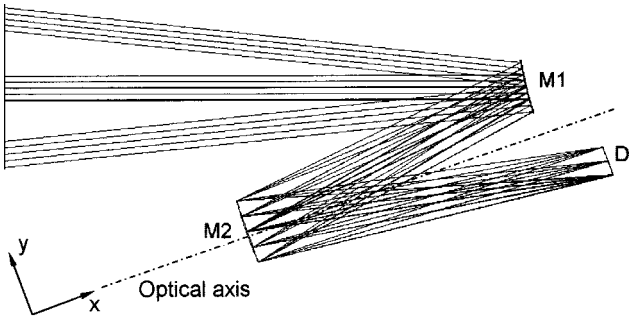

Fig. 1. Optical scheme of the WAC.

signed a quasi-null lens system based on a single refractive optic with spherical surfaces used as compensators. This system, realized by Galileo Avionica (Campi Bisenzio, Italy), has made possible a very successful test of this particular mirror.

2. Wide Angle Camera Optical Design

The WAC of the Rosetta mission adopts an innovative off-axis two-mirror optical configuration.[7] It performs at a diffraction limit over a rather large 12° × 12° field of view (FOV). The optical schematic of the camera is sketched in Fig. 1, and its characteristics are described in Ref. 3. The camera design is based on an off-axis portion of a convex oblate ellipsoidal primary mirror, M1, and a concave oblate secondary one, M2. The parameters for the two mirrors are reported in Table 1. The formula used for defining the conic surface is

$$x(y, z) = \frac{1}{c(k+1)}\left[1 - \sqrt{1-(k+1)c^2r^2}\right], \qquad (1)$$

where $r^2 = y^2 + z^2$, k is conic constant parameter, and $R = 1/c$ is the radius of curvature at the surface vertex. The tolerance analysis performed on the whole WAC design has set M1 shape tolerance values equal to ±0.1 mm on the vertex radius and ±0.03 on the conic constant (see Table 1).

The M1 has been realized by cutting two off-axis mirror portions from an assosymmetric parent mirror of 150 mm diameter; therefore the whole parent mirror had to be polished to optical quality. This mirror was extremely difficult to realize; in fact, the difference at the edges of the substrate between the mirror surface and its best-fit sphere is of the order of 380 μm. This implies the removal of a large amount of glass material and a relatively large local slope. As a consequence, during the fine polishing activity the control of the mirror's optical quality on the glass substrate has to be extremely accurate.

Table 1. M1 and M2 Mirror Characteristics

	Radius or Curvature (mm)	Conic Constant	Shape	Size
M1	406.6 ± 0.1	5.71 ± 0.03	Square	50 mm × 50 mm
M2	400.0 ± 0.1	0.16 ± 0.03	Circular	D = 61 mm

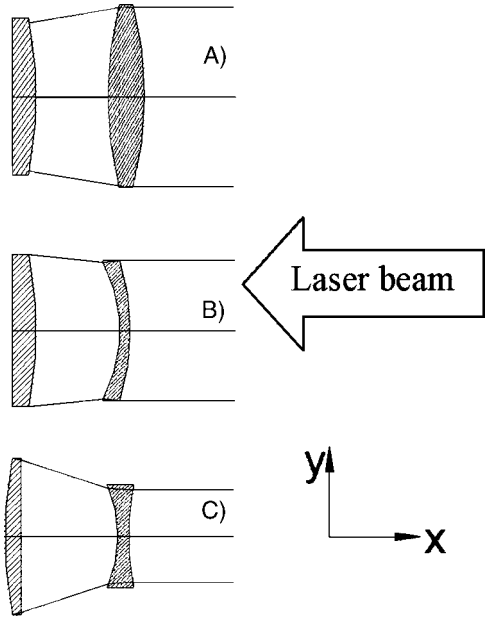

Fig. 2. Possible designs of a null lens setup.

3. Quasi-Null Lens System Design

To achieve an interferometric setup to monitor the optical quality of the 150 mm diameter assosymmetric ellipsoidal parent mirror during the fine-polishing phase, different optical schemes had to be taken into consideration. All the configurations were designed to obtain a null lens system.

In the first scheme [see Fig. 2(a)] a positive lens focuses the laser beam toward the ellipsoidal surface. With this configuration the mirror is tested frontally, and the laser beam is reflected by the mirror surface. Even if rather simple in theory, this classical solution had to be discarded. In fact, simulations performed with a ray-tracing code have shown that the theoretical compensator is a very large aspherical lens, critical to be realized. This fact, together with the high optical quality requirements for this lens, meant that the null lens would have been more difficult and expensive to realize than the mirror itself. Moreover, in this configuration the laser beam diameter should have been larger than what was available from the interferometer.

In the second scheme [Fig. 2(b)], the sample beam is refracted by the null lens, passes through the mirror substrate and is backreflected by the mirror's blank flat surface. In this way, the laser beam size and the null lens are smaller than those necessary in the first scheme. Obviously, to perform this test the rear flat surface of the mirror blank had to be polished to interferometric quality. The results of the simulations showed that the optimal null lens is a meniscus lens with aspherical surfaces; unfortunately, as in the first scheme, this kind of optic requires a great deal of effort to produce.

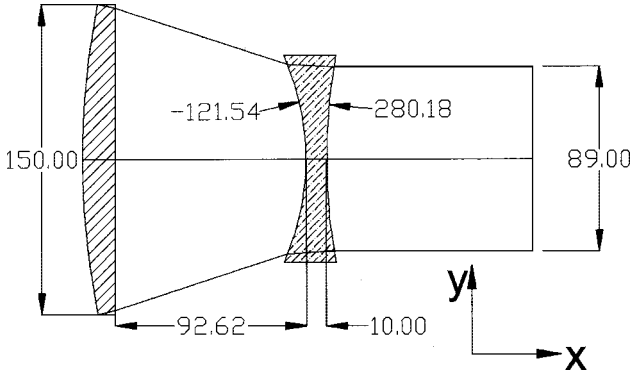

Fig. 3. Project of the quasi-null lens.

Finally, a third solution has been considered, as shown in Fig. 2(c). This scheme is similar in principle to the second scheme, but in this case the mirror is reversed: The laser beam impinges the flat surface, passes through the blank substrate and is backreflected by the surface under test at its concave side. The results from the simulations show that in this design the nominal compensating element is a biconcave lens, also, in this case, with aspherical surfaces. The need to realize aspherical optical surfaces to obtain a null system still remains, but in this last case, in contrast to the others, the lens surfaces do not differ too much from the spherical ones. This fact made us consider the possibility of adopting a quasi-null lens system that is an optical system in which some residual aberrations were still present, but whose relative amount of fringes in the interferogram were rather low. In fact, the knowledge of the fringe pattern from ray tracing allows us to use this method to control the mirror polishing by subtracting in real time this pattern from the interferogram acquired to obtain a null lens synthetic pattern.

In this perspective, the scheme shown in Fig. 2(c) can be realized adopting a biconcave lens with simple spherical surfaces. Since the illuminating beam and the null lens size are also small, this solution has been adopted for testing the mirror surface optical quality. Obviously, the system allows good control of the mirror surface only if the flat rear mirror surface is also polished to interferometric quality level. A sketch of the design of the quasi-null lens system derived by the optimization of the optical scheme just described is shown in Fig. 3. The null lens optical characteristics are summarized in Table 2.

From the simulations performed to evaluate the capability of the system, the interferogram shown in

Table 2. Bi-Concave Quasi-Null Lens Parameters

R_1 (radius of curvature first surface)	−121.54 mm
R_2 (radius of curvature second surface)	280.18 mm
Thickness (at center)	10 mm
Diameter	90 mm
Material	BK7
Distance M1-lens vertex	92.62 mm

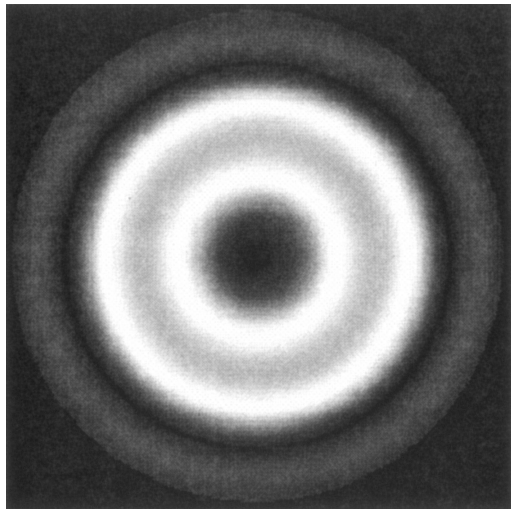

Fig. 4. Theoretical interferogram obtained by simulation.

Fig. 4 has been obtained. The presence of some fringes in the nominal configuration is actually due to the imperfect compensation of the system (i.e., this is a quasi-null lens system). Nevertheless, the system can be efficiently applied to perform the polishing of the mirror once this nominal interferogram is subtracted in real time from the interferometric images acquired. Figure 5 shows the wavefront profile plot of the interferogram itself along a pupil diameter (the system is rotationally symmetric); that residual amount of uncompensated wavefront has a peak-to-valley (PTV) value of only 0.44λ at 632.8 nm. The residual aberration Zernike coefficients, obtained by the interferometric analysis (p is the normalized radial coordinate on the exit pupil of the null lens optical system) are reported in Table 3. As shown, the aberration coefficients are quite small.

Since the ellipsoidal mirror is tested from the back and the radiation is backreflected from the glass side, this system is 1.5 times more sensitive to Δx errors

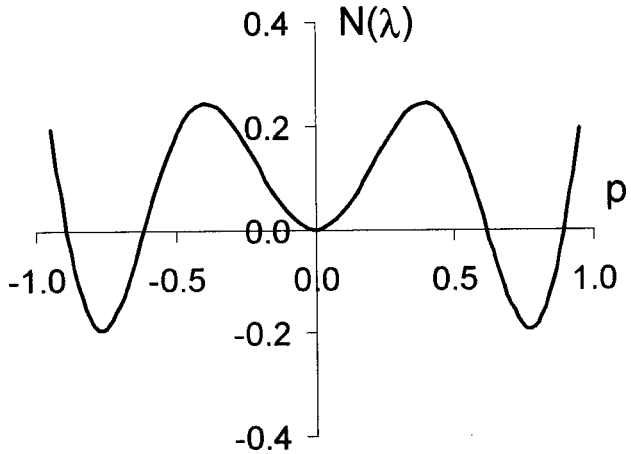

Fig. 5. Optical path difference (measured in wavelengths, where λ = 632.8 nm) with respect to chief ray as a function as the normalized radial coordinate p on the exit pupil of the optical system.

Table 3. Theoretical Values of the Residual Aberrations Expressed in Terms of Zernike Coefficients

	Zernike Coefficients	Nominal
Z_9	$(6p^4 - 6p^2 + 1)$	0.258 λ
Z_{16}	$(20p^6 - 30p^4 + 12p^2 - 1)$	0.217 λ
Z_{25}	$(70p^8 - 140p^6 + 90p^4 - 20p^2 + 1)$	−0.171 λ
Z_{36}	$(252p^{10} - 630p^8 + 560p^6 - 210p^4 + 30p^2 - 1)$	−0.029 λ
Z_{37}	$(924p^{12} - 2772p^{10} + 3150p^8 - 1680p^6 + 420p^4 - 42p^2 + 1)$	−0.003 λ

(for the x axis direction see Fig. 2) then the usual setups in which the illumination of the surface under test comes from the front side, a fact that characterizes this system as a very powerful tool. In fact, let us consider two points, A and B, on a plane wavefront impinging on a BK7 substrate (i.e., our mirror) (see Fig. 6); if a defect of Δx height is present on the back side of the substrate (i.e., the primary surface mirror), the traveling times inside the glass for optical paths A and B are not equal, but they are, respectively, $t_A = 2L/v$ and $t_B = 2(L - \Delta x)/v$, where L is the thickness of the substrate and v is the speed of light in BK7. The optical path difference, as seen by the interferogram, is then

$$s = (t_A - t_B)c = 2\Delta x \frac{v}{c} = 2n\Delta x \cong 3\Delta x. \qquad (2)$$

Therefore the so-called physical wedge factor to be considered in this interferometric analysis is $1/3 = 0.33$, to be compared with the $1/2 = 0.5$ factor used for the front-side setups.

To have a reasonable certainty about the results of the described procedure, a sensitivity analysis of the interferometric setup was also performed by simulating the whole system by using the given mirror tolerances reported in Table 1. This analysis has shown that a change in the M1 radius of ±0.1 mm is essentially equivalent to introducing a spherical aberration in the quasi-null lens system, which can be compensated for by varying the nominal distance between the mirror and the biconcave lens of ±60 μm. This means that the system is indeed rather insensitive to realistic variations of the radius of the parent mirror with respect to the nominal one, and therefore that the radius of the optics has to be measured independently. Conversely, a variation of the conic constant value of ±0.03 is only very partially compensated for by varying the nominal distance between the mirror and the biconcave lens of ±50 μm. This demonstrates that this system is very sensitive to possible variations of the conic constant with respect to the nominal value.

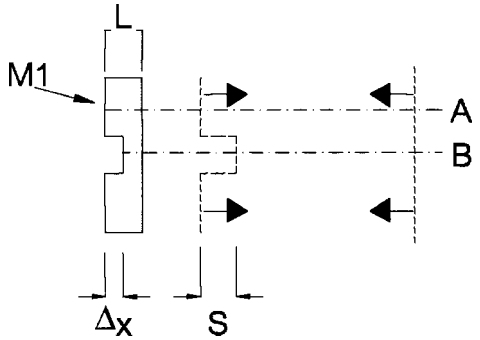

Fig. 6. Optical path difference in the reflected wavefront when illuminating a mirror from the back side.

Table 4. Seidel Aberration Coefficients Evaluated by Interferometric Test of the Biconcave Lens

	First Surface (R_1)	Second Surface (R_2)
Astigmatism	−0.067 λ (at 632.8 nm)	−0.073 λ
Coma	0.056 λ	0.049 λ
Spherical	0.162 λ	−0.035 λ

Tolerances related to the alignment of the interferometric setup have also been investigated. First, it is necessary to observe that all the optical components of the interferometric system have been realized by means of rotationally symmetric machines. This has the consequence that significant nonaxial symmetric aberrations can be present in the system only if there are some misalignments of the optics, such as tilt and/or decentering. Actually, it is possible that the flat back surface of the mirror is not exactly coaxial with the conic front surface, and also in this case some nonaxial symmetric aberrations as coma would be present in principle. However, owing to the requirement of 1 arc min tolerance for the coaxiality between the two mirror surfaces given to the optics producer, the simulations performed have proven that this effect is negligible. Under these hypotheses, it is clear that if some nonaxial aberrations are present in the interferogram when the mirror is under test, the optical elements of the system are not well aligned (for example, it has been verified that a tilt of the lens of 0.01° with respect to the z axis gives

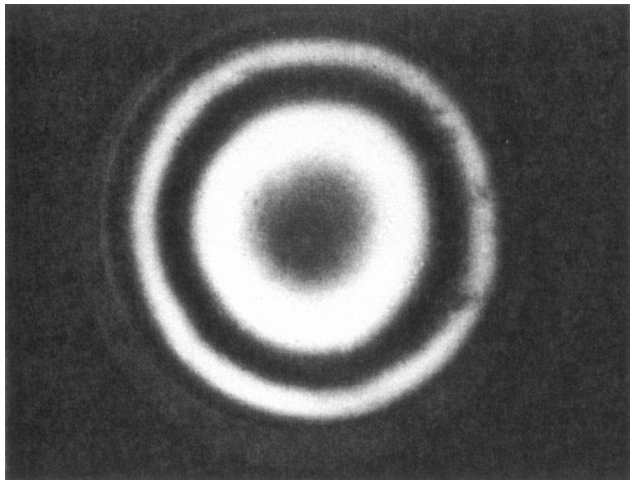

Fig. 7. Interferogram acquired during the polishing phase of one of the mirrors.

Table 5. Zernike Coefficients of One of the M1 Mirrors after Polishing in the Quasi-Null Lens Setup

Z_2	0.227 λ	Z_{11}	0.170 λ	Z_{20}	−0.016 λ	Z_{29}	0.002 λ
Z_3	−0.270 λ	Z_{12}	−0.013 λ	Z_{21}	−0.002 λ	Z_{30}	−0.023 λ
Z_4	−0.151 λ	Z_{13}	−0.051 λ	Z_{22}	0.005 λ	Z_{31}	−0.025 λ
Z_5	−0.015 λ	Z_{14}	0.021 λ	Z_{23}	0.002 λ	Z_{32}	0.046 λ
Z_6	0.210 λ	Z_{15}	−0.012 λ	Z_{24}	−0.005 λ	Z_{33}	−0.051 λ
Z_7	0.046 λ	Z_{16}	0.003 λ	Z_{25}	0.010 λ	Z_{34}	0.022 λ
Z_8	−0.115 λ	Z_{17}	0.089 λ	Z_{26}	0.021 λ	Z_{35}	0.010 λ
Z_9	−0.016 λ	Z_{18}	0.003 λ	Z_{27}	0.044 λ	Z_{36}	0.011 λ
Z_{10}	−0.258 λ	Z_{19}	0.022 λ	Z_{28}	−0.012 λ	Z_{37}	−0.003 λ

a Zernike aberration coefficient of $Z_8 = 0.7$ λ). This means that the interferometer itself can be used to validate the alignment of the setup: The system is optimally aligned when all the nonaxial aberrations are minimized on the interferogram. Owing to the extreme accuracy of the interferometer, this technique allows us to obtain an extremely accurate alignment of the system. Finally, regarding possible misalignments due to nonprecise axial positioning of the optics, we can observe that these translate into defocus and spherical aberrations on the interferogram that are not of interest for this measurement. Since the light must travel inside the mirror substrate, another important factor that could affect the interferogram is the material homogeneity. In this case, a very standard material such as BK7 has been adopted to realize the mirror substrate, and the glass properties have been guaranteed by Schott certification.

4. Quasi-Null Lens Fabrication

The quasi-null biconcave lens has been fabricated and tested by Galileo Avionica, Campi Bisenzio, Italy. The radius of curvature of the two lens surfaces has been measured with a profilometer; the value of the radius of curvature of the first lens surface is $R_1 = 121.58$ mm, against the theoretical value of 121.54 mm, and the radius of curvature of the second lens surface is $R_2 = 280.20$ mm (theoretical value 280.18 mm). These very small variations with respect to the nominal radii do not affect the systems performance, but they require a minor adjustment of the nominal distance between the lens and the mirror to be tested, bringing it to 92.58 mm. In Table 4 the third-order Seidel aberration coefficients related to each one of the spherical surfaces of the biconcave lens obtained by an interferometric analysis are reported. Since the PTV value is 0.198 λ at 632.8 nm, and the rms value on the surfaces is better then λ/20, the error introduced in the interferometric setup by the quasi-null lens can be assumed negligible.

5. Mirror Realization

A total of six M1 mirrors were requested from Galileo Avionica: the two of lowest quality for the WAC breadboard, the two of best quality for the WAC qualification and the flight models, and the remaining two as spares. To realize all these mirrors, three parent mirrors were shaped by a numerically controlled machine (Carl Zeiss Incorporated).

Before beginning the polishing activity, a series of metrological measurements were performed on the mirrors under test, including a measurement of the radius by means of a profilometer, scanning the surface along three different diameters. By fitting the acquired profile with a surface having the nominal conic constant (i.e., 5.71), the radius of the mirrors was established. As already mentioned, a variation of the radius of the parent mirror with respect to the nominal one requires a small adjustment of the dis-

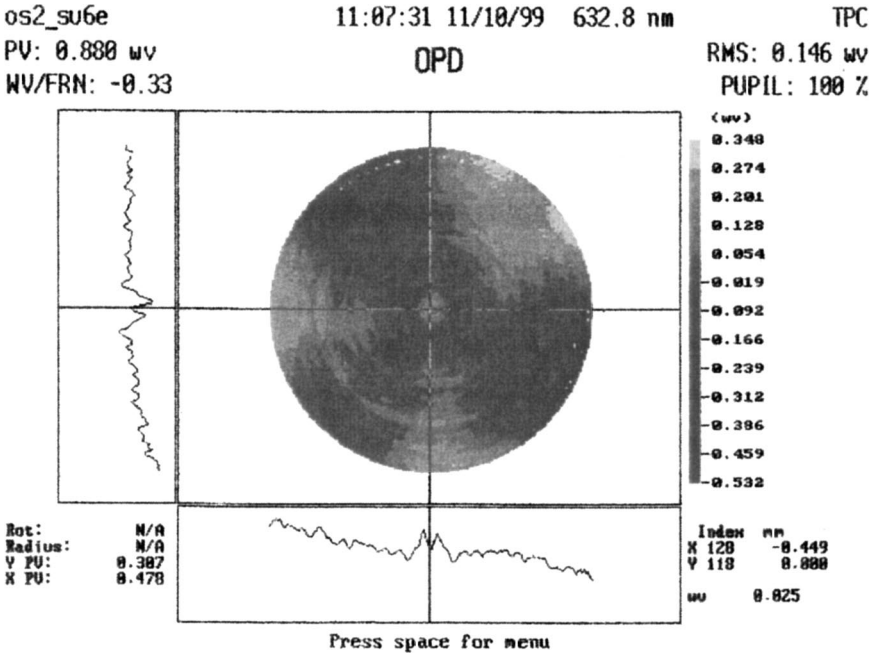

Fig. 8. Interferogram acquired at the end of the polishing phase of one of the mirrors once the synthetic one is subtracted.

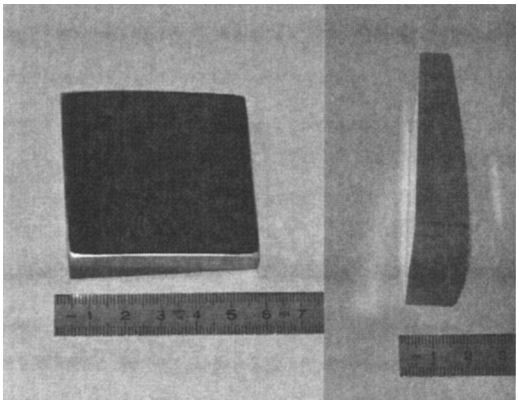

Fig. 9. Image of one of the M1 mirrors.

tance between the mirror itself and the biconcave lens to compensate for the spherical aberration.

At this point the mirrors were polished by using the quasi-null lens setup to monitor their shape. In Fig. 7 the acquired interferogram obtained in one of the polishing sessions is shown to be compared with the nominal one of Fig. 4. In Table 5, the Zernike coefficients corresponding to the postpolishing interferogram of Fig. 8 obtained by removing the synthetic interferogram, are reported: they show a very low amount of aberration residuals, with a PTV of 0.88 λ and an rms value of 0.146 λ. All six mirrors were fabricated by Galileo Avionica within specification (the flight M1 mirror is shown in Fig. 9), a fact that confirms the capabilities of the control method implemented with this simple quasi-null lens system.

For a final and complete verification of the quality of the whole integrated WAC instrument, an interferometric test was performed using a Zygo interferometer (Fig. 10): the collimated beam exiting the interferometer is focused on the focal plane of the camera, once the detector is removed. The beam is then nominally collimated by the two mirrors, and is backreflected inside the camera by a plane mirror placed in a suitable position. It then returns to the interferometer where the interferogram is produced. The residual aberrations measured by the interferogram with this setup are compared with the theoretical ones for the central point of the FOV in Table 6. Thanks to the high quality of the fabricated mirror and to the proper alignment, the optical performances of the WAC have been demonstrated to be

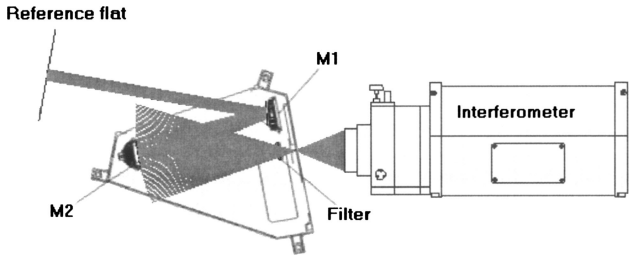

Fig. 10. Setup for interferometric test of the whole WAC by using a Zygo interferometer.

Table 6. Residual Aberrations Evaluated by Interferometric Test in the WAC System for the Central FOV and Theoretical Comparisons

	Experimental	Theoretical
Astigmatism	0.56 λ	0.55 λ
Coma	0.24 λ	0.09 λ
Spherical	−0.25 λ	0.012 λ

extremely good. An extensive presentation of the measured camera performances is reported in Ref. 10. Actually, not only the end-to-end tests performed on the ground, but also the first images acquired with the WAC in flight, show that the optical performances of this instrument is excellent, with an instrument point-spread function at the limit of diffraction.

6. Conclusions

A very innovative, simple, low-cost and reliable quasi-null lens setup has been designed to fabricate a convex oblate ellipsoidal mirror characterized by a relatively high value of the conic constant. The theoretical performances and technological aspects related to the realization of the system have been the object of this study. An experimental setup has been realized to fabricate the primary mirror of the WAC of the OSIRIS instrument onboard the Rosetta ESA mission. This mirror has been successfully realized and tested, and the performance goal of the WAC instrument has been achieved.

The authors acknowledge the assistance of all the OSIRIS team, as this work is just a part of the huge effort in the realization of the whole Rosetta imaging system. This work has been supported by a grant from the Italian Space Agency for the realization of the WAC.

References

1. A. Bar-Num, A. Barucci, E. Bussoletti, A. Coradini, M. Coradini, J. Klinger, Y. Longherin, R. J. Laurence, J. A. M. Mc Donnel, A. Milani, B. Picardi, C. Pillinger, G. Schwen, D. Stoffer, and H. Wänke, *Rosetta Comet Rendezvous Mission, Study Report of ESA,* ESA Publication SCI **93** (1993).
2. V. Da Deppo, G. Naletto, P. Nicolosi, P. Zambolin, M. G. Pelizzo, and C. Barbieri, "Optical performance of the wide-angle camera for the Rosetta mission: preliminary results," in *UV/EUV and Visible Space Instrumentation for Astronomy and Solar Physics,* Proc. SPIE **4498,** 248–257 (2001).
3. G. Naletto, V. Da Deppo, M. G. Pelizzo, R. Ragazzoni, and E. Marchetti, "Optical design of the Wide Angle Camera for the Rosetta mission," Appl. Opt. **41,** 1446–1453 (2002).
4. K. Dohlen, M. Saisse, G. Claeysen, J.-L. Boit, "Optical designs for the Rosetta narrow-angle camera," Opt. Eng. **35,** 1150–1157 (1996).
5. N. Thomas, H. U. Keller, E. Arijs, C. Barbieri, M. Grande, P. Lamy, H. Rickman, R. Rodrigo, K.-P. Wenzel, M. F. A'Hearn, F. Angrilli, M. Bailey, M. A. Barucci, J.-L. Bertaux, K. Brieß, J. A. Burns, G. Cremonese, W. Curdt, H. Deceuninck, R. Emery, M. Festou, M. Fulle, W.-H. Ip, L. Jorda, A. Korth, D. Koschny, J.-R. Kramm, E. Kührt, M. L. Lara, A. Llebaria, J. J. Lopez-Moreno, F. Marzari, D. Moreau, C. Muller, C. Murray, G. Naletto, D. Nevejans, R. Ragazzoni, L. Sabau, A. Sanz, J.-P. Sivan, and G. Tondello, "OSIRIS-The optical, spectroscopic

and infrared remote imaging system for the Rosetta orbiter," Adv. Space Res. **21,** 1505–1515 (1998).
6. H. U. Keller, C. Barbieri, P. Lamy, H. Rickman, R. Rodrigo, K.-P. Wenzel, M. F. A'Hearn, F. Angrilli, M. Angulo, M. E. Bailey, P. Barthol, M. A. Barucci, J.-L. Bertaux, G. Bianchini, J. A. Burns, J. M. Castro, G. Cremonese, W. Curdt, S. Debei, M. De Cecco, M. Fulle, F. Gliem, S. F. Hviid, W.-H. Ip, L. Jorda, D. Koschny, J. R. Kramm, E. Kührt, L.-M. Lara, A. Llebaria, J. Lopez-Moreno, F. Marzari, G. Naletto, G. Rousset, L. Sabau, A. Sanz, H. Sierks, J.-P. Sivan, U. Telljohann, N. Thomas, and G. Tondello, "OSIRIS - The optical, spectroscopic, and infrared remote imaging system," submitted to Space Sci. Rev. (2006).
7. R. Ragazzoni, G. Naletto, C. Barbieri, and G. Tondello, "An optical design for the Rosetta Wide Angle Camera," in *Space Telescopes and Instruments,* Proc. SPIE **2478,** 257–268 (1995).
8. D. Malacara, *Optical Shop Testing* (Wiley, 1978).
9. Y. S. Kim, B. Y. Kim, and Y. W. Lee, "Design of null lenses for testing of elliptical surfaces," Appl. Opt. **40,** 3215–3219 (2001).
10. V. Da Deppo, G. Naletto, P. Nicolosi, P. Zambolin, M. De Cecco, S. Debei, G. Parzianello, P. Ramous, M. Zaccariotto, S. Fornasier, S. Verani, N. Thomas, P. Barthol, S. F. Hviid, I. Sebastian, R. Meller, H. Sierks, H. U. Keller, C. Barbieri, F. Angrilli, P. Lamy, R. Rodrigo, H. Rickman, and K. P. Wenzel, "Preliminary calibration results of the Wide Angle Camera of the imaging system OSIRIS for the Rosetta mission," in *Proceedings of the International Conference on Space Optics (ICSO)* (ESA-SP, 2004), pp. 191–198.